Environmental heterogeneity patterns plant species richness and turnover in two hyperdiverse floras

Running title: Environmental heterogeneity and plant species richness

Ruan van Mazijk, Michael D. Cramer & G. Anthony Verboom

Department of Biological Sciences, University of Cape Town, Rondebosch, South Africa

Corresponding author: RVM (ruanvmazijk@gmail.com, +27 21 650 3684)

ORCID nos.: RVM: 0000-0003-2659-6909, MDC: 0000-0003-0989-3266, GAV: 0000-0002-1363-9781

1 # Abstract

2 **Aim:** To quantify the explanatory power of heterogeneity in predicting plant species richness and turnover here
3 in the Greater Cape Floristic Region and in the Southwest Australia Floristic Region. We compare the
4 environmental heterogeneity in each region, how species richness and turnover interact in each region to
5 produce the observed patterns of richness, and what different forms of environmental heterogeneity better
6 predict richness in each region. We expect the Cape to be more heterogeneous in most environmental axes, and
7 at a finer grain, such that the consequent high levels of species turnover explain the Cape's greater species
8 richness per unit area. We also conjecture that edaphic heterogeneity will be an important factor in predicting
9 richness in S.W. Australia.

10 **Location:** The Greater Cape Floristic Region in southwest Africa (the Cape), and the Southwest Australia
11 Floristic Region (SWA)

12 **Taxon:** Vascular plants

13 **Methods:** Geospatially explicit floral and environmental data, non-parametric statistics, boosted regression
14 tree modelling

Results: The Cape is more environmentally heterogeneous and has higher levels of floristic turnover than SWA. We find that environmental heterogeneity is the main predictor of species richness in the Cape, and somewhat less so for SWA. Edaphic conditions are found to be of more biologically important in the Cape, though this is contingent on the quality of the data modelled.

Main conclusions:

Keywords: biodiversity, environmental heterogeneity, fynbos, Greater Cape Floristic Region, kwongan, macroecology, species richness, species turnover, vascular plants, Southwest Australia Floristic Region

Acknowledgements

1 Introduction

Biodiversity represents the variety of living things, and the variety of ecological and evolutionary processes responsible for it (Bøhn & Amundsen, 2004). Studying the distribution of biodiversity in space is a major avenue of biological research (**???**; Kreft & Jetz, 2007). Regional-scale geographic patterns in species richness have long been studied, particularly in biodiversity hotspots (Cook et al., 2015). The spatial distribution of species richness can be explained in terms of the physical environment. Properties of the environment have been suggested to influence species richness in three ways: (i) productivity, water, and energy to enable organismal growth, and resources (i.e. niche space) to support a wider range of species (Gaston, 2000; Kreft & Jetz, 2007; Mouchet et al., 2015); (ii) stability, which enables species' persistence; and (iii) heterogeneity, which enables ecological speciation and possible barriers to gene flow, and with a wider variety of environments to facilitate species' co-existence (Thuiller et al., 2006; Mouchet et al., 2015; Cramer & Verboom, 2016). The physical environment, then, can be used to explain species richness in a

41   local-deterministic sense, and in a historical context (Ricklefs, 1987).

42   The maintenance of species richness, particularly the coexistence of high numbers of species in biodiversity

43   hotspots, is often regarded as "paradoxical" (Hart et al., 2017), and is a central problem in ecology (Ricklefs,

44   1987; Kreft & Jetz, 2007; Hart et al., 2017). Species richness is constrained by the ability of habitats to support

45   a variety of species—its ecological carrying capacity (Mateo et al., 2017). This is exemplified in approaches to

46   modelling species richness as a function of environmental predictors in a correlative framework

47   ("macro-ecological models"; Mateo et al., 2017). Macroecological models of species richness implicitly

48   assume that communities are saturated, following species-area and species-energy relationships, and at

49   equilibrium with the environment (Mateo et al., 2017).

50   A solution to the paradox of species coexistence is environmental heterogeneity (EH): a more heterogeneous

51   environment has a larger environmental space, and can thus facilitate co-existence between species at the scale

52   of that heterogeneity. EH can also stimulate ecological speciation, should the region be environmentally stable

53   over evolutionary time-scales. Heterogeneity in the physical environment is known to be positively associated

54   with species richness (Rensburg et al., 2002; Hart et al., 2017), and has been demonstrated to do so across

55   many taxa—e.g. Canadian butterflies (**???**), European vertebrates (Mouchet et al., 2015), South African birds

56   (Rensburg et al., 2002), in communities along marine continental margins (Levin et al., 2010), French scarab

57   beetles (Lobo et al., 2004), and for global terrestrial plants (Kreft & Jetz, 2007). The spatial scale of

58   heterogeneity, or "grain" of the environment, is important to consider (Hart et al., 2017), in the same way that

59   the spatial of absolute environmental conditions has also been considered (**???**; Baudena et al., 2015; Mouchet

60   et al., 2015). Species co-existence and biodiversity maintenance is indeed suggested to be scale-dependent

61   (Hart et al., 2017).

62   EH is often under-represented in macro-ecological models of species richness, and has recently been found to

63   explain up to ca. 95% of biome level species richness across South Africa (Cramer & Verboom, 2016). Models

64   that include EH yield better estimates of the richness of the Cape flora, as they account for the role

65   heterogeneous environments such as those in the Cape facilitate species coexistence (Thuiller et al., 2006;

66   Cramer & Verboom, 2016). Mediterranean-type terrestrial biodiversity hotspots, such as the Cape flora

67   included in the models by Cramer & Verboom (2016), present interesting study systems in which to investigate

68   the relationship between the environment and species richness. These systems exhibit far greater species

69   richness than predicted by their areas, productivities and latitudes (Cowling et al., 1996; Kreft & Jetz, 2007).

70   There are five Mediterranean biodiversity hotspots on Earth: the California Floristic Province, the

71 Mediterranean Basin, the Chilean Winter Rainfall-Valdivian Forests, the Greater Cape Floristic Region, and the

72 Southwest Australia Floristic Region (Cowling et al., 1996; Hopper & Gioia, 2004; Cook et al., 2015). These

73 ecosystems have regular fire-cycles (Cowling et al., 1996), climatic buffering, and long term stability (Kreft &

74 Jetz, 2007), shrubby, sclerophyllous flora (Hopper & Gioia, 2004). Together, they account for ca. 20% of

75 global vascular plant species, yet only ca. 5% of global land surface areas (Cowling et al., 1996). Various

76 hypotheses have been proposed to explain the high levels of plant species richness in these regions (Cook et al.,

77 2015). The species accumulation hypothesis states that the stability of these regions has allowed many species

78 to accrue. The species co-existence hypothesis states that these hotspots may facilitate greater degrees of

79 species co-existence in smaller spatial areas, due to fine-scale heterogeneity in their environments. Indeed, EH

80 has evolutionary implications too, stimulating ecological speciation across sharp environmental gradients.

81 Both the Southwest Australia Floristic Region (SWA) and the Greater Cape Floristic Region (Cape) are

82 Mediterranean-type biodiversity hotspots, particularly in terms of plant species. Where the Cape (with an area

83 of ca. 189,000 km^2) is known to contain about 11,400 plant species (about 0.060 species per km^2), SWA (area

84 of ca. 270,000 km^2) has about 3,700 species (0.014 species per km^2) (**???**). So, the Cape has ca. 4.3 times as

85 many species per km^2 as SWA. The Cape and SWA are appropriately often compared, due to the similarities

86 between their environments (e.g. oligotrophic soils, an oceanically buffered moderate climate) and their plants'

87 ecologies (Hopper & Gioia, 2004). These two regions present unique flora out of the five Mediterranean

88 systems, with high levels of endemism (Cowling et al., 1996), and many obligate fire-adapted species (Cowling

89 et al., 1996). Similarities withstanding, SWA is topographically and edaphically distinct from the Cape. The

90 former is topographically rather uniform (i.e. flat)—uniquely so among the world's five Mediterranean-climate

91 regions (Hopper & Gioia, 2004)). SWA possesses a mesoscale chronosequence dune system (Laliberte et al.,

92 2014; Cook et al., 2015), while the Cape is mountainous, topographically heterogeneous, and therefore

93 associated with a large degree of spatial climatic variability, with a fine-scale mosaic of geologies and soils

94 (Cowling et al., 1996; Cramer et al., 2014; Verboom et al., 2017).

95 Both regions have sources of edaphic heterogeneity, but at different scales. This edaphic variability may aid in

96 explaining the species richness in these regions (Beard et al., 2000; Verboom et al., 2017). EH can stimulate

97 ecological speciation, should the region be stable over evolutionary time-scales, as is likely the case in both the

98 Cape and SWA (Wardell-Johnson & Horwitz, 1996; Hopper & Gioia, 2004; Lambers et al., 2010; Cramer et al.,

99 2014; Laliberte et al., 2014; Cook et al., 2015). For the Cape, this richness is largely known to result from long

100 term climatic stability, and fine grain variation in geology and soils (Cramer et al., 2014). The question thus

101 arises whether heterogeneity is a significant contributor to SWA species richness as is likely the case in the

4

Cape. In the absence of topographic variability in SWA, it is proposed that the heterogeneity of that region is due to the juxtaposition of soil types (Laliberte et al., 2014; Cook et al., 2015), creating extreme edaphic variation.

1.1 Hypothesis-v1

Our main hypothesis is that the greater abiotic heterogeneity in the Cape, and the finer grain of that heterogeneity, compared to that of the SWA, accounts for the Cape's greater species richness per unit area. We expect the relationships between EH, species richness, and species turnover in these two regions to demonstrate this. As stated above, heterogeneous environments can (i) support diverse species assemblages, and (ii) stimulate ecological speciation. Thus, we expect species richness to covary with heterogeneity. Additionally, as one moves across a heterogeneous landscape, we expect to find greater turnover in community composition, as different environments support different species. Thus, areas of greater turnover should also be more rich, due to potential complementarity between neighbouring communities increasing total richness. Consequently, we expect that EH positively influences species richness and species turnover, and that species turnover itself positively influences species richness.

1.2 Hypothesis-v2

Aim: This study investigates the role EH plays in explaining vascular plant species richness in the Cape and SWA. We compare the relative importance of heterogeneity between the two regions, as heterogeneity has the evolutionary role of facilitating speciation, and the ecological role of supporting diverse species assemblages. Spatial scale of that heterogeneity is also considered, as the heterogeneity-richness relationship can vary with habitat grain-size.

Our hypotheses concern the Cape and SWA's environments and floras. Our main hypothesis is that the Cape possesses greater abiotic heterogeneity, and at finer grain, compared to SWA, such as to explain the Cape's greater species richness per unit area, and proposed greater levels of species turnover between areas. We also conjecture that the heterogeneity that predicts species richness in SWA will be more pronounced in terms of edaphic variables. Here we attempt to assess six key predictions of this hypothesis, additionally investigating a seventh prediction to test the conjectured role of edaphic heterogeneity in SWA. Dealing with the two regions' environments, we assess (i) whether the Cape environment is more heterogeneous than that of SWA and (ii)

129 whether the Cape environment has more pronounced heterogeneity at finer scales than that of SWA. Dealing

130 with the distribution of species in the two regions, we assess (iii) whether the Cape exhibits greater levels of

131 species turnover between areas. Relating each regions' environment and flora, we finally assess (iv) whether

132 species richness and species turnover are adequately predicted by EH in both regions and whether (v) Species

133 richness and species turnover are better predicted by different forms of EH in either region (e.g. the importance

134 of edaphic heterogeneity in SWA).

135 …

136 We employ classical statistical methods to analyse publicly available geospatial and species occurrence

137 datasets.

138 …

139 Species distribution models (SDMs), or environmental niche models, are sets of empirical methods that relate

140 observed species presences (or similar data) to environmental and spatial variables, often correlatively (Guisan

141 & Thuiller, 2005). As SDMs rely chiefly on correlating observed species ranges with the conditions thereof,

142 they provide only a model of the realised niche of a species (Raes, 2012), which can cause issues when

143 attempting to predict responses of species to changing climate. Other assumptions of typical SDMs include that

144 the range of species considered is in equilibrium with the environment (Altwegg et al., 2014; Guisan & Thuiller,

145 2005; Hannah et al., 2005), thus limiting the efficacy of these models on dynamically ranged or highly vagile

146 species (Hannah et al., 2007). Regardless, given the dynamic nature of biotic ranges under climate change,

147 SDMs are a valuable tool in identifying the contemporary risks posed to global and regional biodiversity.

148 The GCFR is a megadiverse terrestrial biogeographic region, with high levels of endemism. Midgley et al.

149 (2003) investigated the responses the now defunct Cape Floristic Region (CFR) flora to climate change. Using

150 bioclimatic envelope models (a form of SDM), they modelled the Fynbos Biome's distribution as a whole, and

151 select Cape-endemic Proteaceae species' distributions, under current and future climate (climate scenario

152 HadCM2), and again with the impact of land use change. Their Fynbos model was an indicator of regional

153 priority for species level modelling efforts, showing a general southwards contraction of the biome. Their

154 specific Proteaceae models yielded various results: complete extinctions for some species, range contractions

155 for most, improbable range shifts in some, and range expansions in few. The range shifts predicted therein were

156 acknowledged to be improbable, due to the unmodelled limitations of plant dispersal and edaphic dependence.

157 Midgley et al. (2003) concluded that climate change is likely to have severely negative for the CFR flora.

158   However, as will be outlined below, their methods may be overpredicting losses due to climate change.

159   …

160   The last 20 years have seen much ecological research interest in and development of SDMs, using many
161   statistical and machine-learning-based methodologies (Altwegg et al., 2014; Elith et al., 2008, 2011; Guisan &
162   Thuiller, 2005). Machine-learning-based methods in SDMs include MaxEnt (Elith et al., 2011), genetic
163   algorithms, and adaptive neural networks (Hannah et al., 2005). The use of more advances statistics
164   (e.g. Bayesian frameworks, ordination methods (Hannah et al., 2005)) is also seen. These two avenues of
165   research have intersected in the development of boosted regression trees (BRTs) (originally "gradient boosting
166   machine"; Friedman, 1999) a system of recursively generated, non-linear regression trees, as outlined by Elith
167   et al. (2008). BRTs have been used as SDMs in southern Africa before (e.g. Thuiller et al., 2006), sometimes
168   for conservation purposes (e.g. Coetzee et al., 2009), but BRTs have yet to be used specifically to assess the
169   responses of the regional flora to climate change. BRTs have more flexibility in their predictions than more
170   traditional methods (e.g. GAMs), as they are non-linear and machine-learning-based (Elith et al., 2008).

171   …

172   ## 2   Materials and methods

173   ### 2.1   Overview

174   Our analyses required definitions of the boundaries of the two regions, environmental data for each, and
175   geospatially-explicit vascular plant occurrence records, all based on publicly available data. The environmental
176   variables chosen (Table 1) for this study were intended to cover a reasonable spread of climatic, edaphic, and
177   ecologically relevant environmental axes, and are not intended to be exhaustive. We selected variables
178   describing topography (elevation), productivity (NDVI), soil status, and climate and climatic seasonality.

179   We carried out this investigation at four principal spatial scales: 0.05º x 0.05º squares (the finest common
180   resolution among the environmental data sources used), quarter degree squares (QDS) (Larsen et al., 2009),
181   half degree squares (HDS) (Larsen et al., 2009) and three-quarter degree squares (3QDS). For the Cape, most
182   plant occurrence records are only accurate to QDS level. Thus, any analysis involving species data was
183   necessary limited to scales above and including QDS.

184 Analyses were performed in R v3.4.0–3.5.1 (R Core Team, 2018). Version-numbers of specific R packages

185 used are presented in the bibliography.

186 ## 2.2   Environmental data sources

187 Geospatially-explicit raster layers were acquired for a selection of environmental variables (Table 1), for the

188 regions of interest. Here, the GCFR was treated as the areas occupied by the Succulent Karoo and Fynbos

189 biomes in the current delineation of South Africa's biome boundaries (Mucina & Rutherford, 2006). The

190 SWAFR was treated as the areas occupied by the Southwest Australia savanna, Swan Coastal Plain Scrub and

191 Woodlands, Jarrah-Karri forest and shrublands, Southwest Australia woodlands, Esperance mallee, and

192 Coolgardie woodlands in the World Wildlife Fund Terrestrial Ecoregions dataset (Olson et al., 2001) in order to

193 closely match the currently delineated SWAFR (Gioia & Hopper, 2017, Hopper & Gioia (2004)). For the sake

194 of readability, we shall refer to the GCFR and SWAFR simply as the Cape and SWA from hereon.

195 Raster data were re-projected to a common coordinate reference: WGS84 (NIMA, 2000), using the "rgdal"

196 (**???**) package in R (R Core Team, 2018). All data were re-sampled to 0.05º resolution using the "resample"

197 function in the R package "raster" (**???**), with the "bilinear" method.

198 An emphasis was made on using satellite-derived environmental data in this work, in order to minimise

199 differences in data quality and methodologies between the Cape and SWA. Additionally, satellite-derived data

200 have been shown to benefit regional-scale species distribution models (Deblauwe et al., 2016), thus motivating

201 their use in this regional-scale study. The environmental data used in this study were derived from NASA's

202 SRTM digital elevation model (Farr et al., 2007), NASA's MODIS/Terra spectroradiometric data for land

203 surface temperature and NDVI, the Climate Hazards Group's CHIRPS rainfall dataset (Funk et al., 2015), and

204 the International Soil Reference and Information Centre's SoilGrids250m edaphic dataset (Hengl et al., 2017)

205 (Table 1). SRTM and MODIS are entirely derived from satellite measurements, whereas CHIRPS is

206 interpolated from weather station data with satellite-derived radiometric measurements. SoilGrids250m is a

207 machine-learning derived product, based on soil measurements as a function of many covariates, including

208 MODIS and STRM sources (see Hengl et al., 2017), using random-forests and other classification-tree-based

209 methods, including gradient-boosting. For the soil data considered here (Table 1), we used depth-interval

210 weighted average values as the value for a particular soil variable in a given place.

211 Climatic and spectral data arise from satellites monitoring properties of the Earth's surface through time. We

212 therefore use the mean annual values for rainfall, surface temperature, and NDVI in each pixel in our analyses.

213 Pronounced seasonality of rainfall is a known feature of Mediterranean systems (**???**). We describe this

214 seasonality by computing computing the precipitation in the driest quarter (PDQ), using code from within the

215 "biovars" function in the R package "dismo".

2.3   Plant occurrence data

217 Geospatially-explicit records of vascular plant occurrences were downloaded from the Global Biodiversity

218 Information Facility (GBIF, Table 1). Queries were made for tracheophyte records from within the borders of

219 the Cape and SWA as treated here (GBIF, 24 July 2017, GBIF (24 July 2017)). Only records with defined

220 species and intra-specific ranks were kept. Intra-specific occurrences were treated as simply being

221 representative of their species. This resulted in FIXME unique species names in the Cape, and FIXME in SWA.

222 We cleaned these data using the R package "taxise" (**???**, (**???**)) to check that these species names had

223 accepted-status among taxonomic databases. I queried two major taxonomic databases: the Global Name

224 Resolver (GNR), and the Taxonomic Name Resolution Service (TNRS). Should one of either service return at

225 least one match for a given name, then that name was deemed accepted. Those names for which no full

226 binomial matches were found in either database were excluded from the final list of species. The number of

227 species names excluded totalled at FIXME and FIXME for the Cape and SWA respectively. Especially for

228 SWA, these numbers may be deemed appreciably high. But, the occurrence records that would be dropped, as a

229 consequence of these names' removals, seemed to be distributed randomly in geographic space in both regions.

230 As such, any effect of the loss of these records in this analysis is uniform within the two regions.

231 After the unaccepted names were removed, it was important to ensure that a species was not listed under

232 multiple synonyms. Such cases would skew the species richness data used in this study. In light of this, the

233 remaining names were queried in the Tropicos and Integrated Taxonomic Information System (ITIS) databases

234 for their known synonyms, using "taxize". These were collated to produce a nomenclatural "thesaurus" for the

235 Cape and SWA species. This consisted of a list of the accepted species names in a region, each associated with

236 a list of known synonyms. I amended species' names in the GBIF occurrence data, in order ensure species were

237 listed under only one of these synonyms, as follows: For each entry in the thesaurus, for each synonym of that

238 entry, if that synonym appeared in the GBIF species list, I replaced all appearances of that synonym in the

239 species list with the original name from the thesaurus-entry that that synonym came from.

240 Lastly, I removed any species from both regions that are invasive aliens or non-indigenous. Alien species lists

241 for plants in South Africa and Australia were acquired from the IUCN's Global Invasive Species Database

242 (http://www.iucngisd.org/gisd/).

243 The final total plant species richness in each region was FIXME and FIXME for the Cape and SWA

244 respectively. These final collections of species occurrence records were converted to raster-layers, wherein

245 pixel-values represented the species, genus and family richness of vascular plants within that pixel. These

246 rasters were produced at QDS, HDS, and 3QDS resolutions.

2.4 Analyses

2.4.1 Quantifying environmental heterogeneity

249 First, in order to assess predictions (i) and (ii), we needed to describe the EH in both regions. Using the R

250 package "raster" (**???**), we used a modified version of the "roughness" index in the "terrain" function. For a

251 three by three neighbourhood $\mathbf{N}$ of cells, our index of roughness R is the average square-root of the squared

252 difference between each of the n neighbour cells' values x_i and the central focal cell's value x_{focal}:

$$R(\mathbf{N}) = \frac{1}{n} \sqrt{\sum_{i=1}^{n} \left(x_{\text{focal}} - x_i\right)^2} \tag{1}$$

253 This value, notionally the standard deviation of values relative to the focal value, is ascribed to the focal cell.

254 Note, in order to use as much data from within regions' borders as possible, roughness was computed if a focal

255 cell had at least one neighbour cell—that is, roughness is defined where $n_{x_{\text{focal}}} \geq 1$. Using this index of

256 heterogeneity, we produced raster layers of each of our nine environmental variable's heterogeneity. We

257 compared the distributions of roughness values in each variable in each region with non-parametric

258 Mann-Whitney U-tests, as almost all variables could not be normalised by log-transformations. We also

259 compare the effect size of the Cape vs SWA using the "common language effect size" ($CLES$), using the R

260 package "canprot". The $CLES$ is the proportion of all pairwise comparisons between two sample groups'

261 observations where one group's value is greater than the other. In our case, of all pairwise comparisons of a

262 variable's roughness values between the Cape and SWA, we calculated the $CLES$ as the proportion of pairs

263 where Cape roughness values were greater than that of SWA. This allowed us to assess prediction (i). To

264 compare the spatial scales of heterogeneity (prediction (ii)) between each region, we repeated this analysis at

265 all four spatial scales. Once again, this entailed recalculating the roughness layer for each variable after the

266 original layer (0.05 degrees resolution) had been rescaled to each of the coarser resolutions.

2.4.2 Quantifying species turnover

268 Regarding prediction (iii), we wished to compare the general degree of species turnover in each region. To

269 compare the extent of species turnover between the Cape and SWA, we determined two metrics of species

270 turnover. The first, computes the mean species turnover as Jaccard distance (**???**) between each pair of QDS

271 within each HDS ($\overline{J}_{\mathrm{QDS}}$, based on HDS with $2 \leq n \leq 4$ QDS) in both regions. The second is defined in terms

272 of Whittaker's additive definition of β-diversity (**???**), as follows:

$$\gamma = \alpha + \beta \tag{2}$$

273 Here, we treat species richness at the HDS-scale (S_{HDS}) as γ-diversity and at the QDS-scale as α-diversity.

274 Intuitively, the species richness of an area is the result of the richness of sites within that area and the difference

275 in species complements between those sites.

276 Thus, we use here an additively defined residual turnover (T_{HDS}; i.e. $\beta = \alpha - \gamma$) as the proportion of S_{HDS}

277 unexplained by the mean species richness of HDS' constituent QDS ($\overline{S}_{\mathrm{QDS}}$).

278 Thus, we partition γ-diversity as in Equation (2), such that β-diversity is the difference between γ- and

279 α-diversity.

280 We compare the distributions of $\overline{J}_{\mathrm{QDS}}$ and T_{HDS} using non-parametric Mann-Whitney U-tests, in order to

281 guard against non-normality.

2.4.3 Predicting richness and turnover with environmental heterogeneity

283 Regarding prediction (iii), we wished to compare the general degree of species turnover in each region. For (iv)

284 and (v) we modelled species richness (S) and turnover as a function of various combinations of environmental

285 and environmental heterogeneity variables in both regions using boosted regression-tree (BRT) modelling

286 techniques. Allowing us to explore which axes of environmental heterogeneity have most influence on vascular

287 plant species richness and turnover, and the differences in the importance of such axes between the Cape and

288   SWA.

289   BRTs are a flexible machine learning-based model of response variables and do so without involving normal

290   null-hypothesis significance testing (Elith et al., 2008), and have been employed previously to model species

291   richness (Thuiller et al., 2006; see Mouchet et al., 2015; Cramer & Verboom, 2016) as macro-ecological

292   models. BRTs are developed through the iterative generation of non-linear regression trees. BRTs are an

293   ensemble-approach, in which a prediction $\widehat{y_i}$ is based on the weighted sum of the predictions of progressively

294   "less important" regression trees (t_k), as opposed to the predictions of one tree (Elith et al., 2008). For $k \rightarrow nt$

295   number of trees, where each tree is itself a function of the matrix $\mathbf{X}$ of j predictor variables ($t_k = f(x_{ij})$), a

296   BRT-model can be represented as follows:

$$\widehat{y_i} = \sum_{k=1}^{nt} w_k t_k \tag{3}$$

297   BRTs have two major meta-parameters that users have control over (**???**): the learning rate (lr, the rate at

298   which iterative trees reduce predictive deviance during model-training, conceptually a "shrinkage factor"

299   controlling the contribution of each tree to the final model) and tree complexity (tc, the number of nodes on a

300   given regression-tree, i.e. the maximum interaction depth the model is permitted to fit).

301   BRTs were implemented here to predict both vascular plant species richness and turnover in each HDS, as a

302   function of environmental variables and environmental roughness values in those cells, as Gaussian responses,

303   thus resulting in two BRT-models for each region. We treated richness as S_{HDS} and turnover as $\overline{J}_{\mathrm{QDS}}$. The

304   natural logarithm of species richness was used, in order to satisfy the assumptions of a Gaussian response.

305   Note, this is not strictly because BRTs have any parametric assumptions concerning the distribution of the

306   response variable, but rather to aid in applying the Gaussian-family of BRT algorithms to the richness data

307   available. Additionally, BRTs were implemented to predict both vascular plant species richness at the

308   QDS-scale (S_{QDS}), thus resulting in a total of six BRT-models presented here.

309   As recommended by Elith et al. (2008), BRT models were trained on a set of non-collinear predictor variables

310   using "gbm.step" in "dismo" (**???**) and "gbm" (**???**). Collinear predictor variables can skew the interpretation

311   of results, as the relatively influence of mutually collinear variables is reduced. Collinearity among the 9

312   environmental predictor variables and their respective 9 roughness-equivalents was assessed using

313   "removeCollinearity" in the R package "virtualspecies" (**???**) separately for each region, such that variables

314   were no more than 80% collinear (Pearson's $r \geq 0.80$). When faced with a cluster of collinear variables, one

315 variable was chosen manually therefrom. Where possible, the roughness-equivalent of an environmental

316 variable was included if its absolute-equivalent could also be included. When interpreting the results of BRTs,

317 it is important to consider the effects of the variables included as representative of the effect of the excluded

318 variables with which it is collinear.

319 In order to select ideal lr and tc all models (described below) were trained on the final non-collinear predictor

320 sets iteratively for 25 combinations of a range of tc values (1 to 5) and a range of lr values (0.01, 0.005, 0.001,

321 5×10^{-4}, 1×10^{-4}). The function "gbm.step" optimises the number of trees (nt) using cross-validation during

322 model training (Elith et al., 2008) by halting iteration when predictions begin to overfit. For all models, we

323 used 10 cross-validation folds (i.e. use 10 different randomly selected training data sets), a tolerance-threshold

324 of 0.001, a bagging-fraction of 0.75 (proportion of training data randomly chosen to generate each tree), and

325 trained models starting with 50 trees, with each iterative step adding 50 trees at a time, up to a maximum of

326 10,000 trees. Following this iterative parameter optimisation, Gaussian BRT models were constructed with

327 $tc = 3$ and $lr = 0.001$, along with the other settings described.

328 BRT-model performance can described by measuring the variance in a dataset a BRT-model has explained,

329 quantified here by R^2_{pseudo}, which is the proportion of null deviance D_{null} explained by some model i.

330 Formally, it is defined as follows:

$$R^2_{\text{pseudo}} = 1 - \frac{D_i}{D_{\text{null}}} \tag{4}$$

331 This metric does not always yield easy interpretation, though, as it is not immediately clear what model

332 deviance is. Alternatively, comparing expected (i.e. model-predicted) and observed data has more heuristic

333 appeal. We employed this metric of BRT-model performance too. We regressed expected against observed

334 richness and turnover, and calculated the R^2-value for those regressions (hereafter $R^2_{\text{E}-\text{O}}$).

335 The BRT-model fitting algorithm has some intrinsic stochasticity because of the random partitions made in a

336 dataset during cross-validation. Though this randomness is usually negligible (e.g. variables' contributions

337 vary from run-to-run by a few decimal places), we ran each of the six BRT-models (see above) 1000 times in

338 order to account for this stochasticity. Where indicated, we either present the average these replicate-models'

339 results or the results of a representative model from each set of replicates.

340 In order to assess the reliability of the conclusions drawn from these models, we randomly permuted the

341 response data (S_{QDS}, S_{HDS} and $\overline{J}_{\text{QDS}}$) with respect to the environmental and heterogeneity data, and refit all

342   six BRT-models 999 times (with the final non-collinear predictor sets and preconfigurations above). This also

343   allows us to remove any effect of spatial autocorrelation in generating the observed correlations between

344   patterns of species occurrence and environment (**???**), and to allow us to assess the significance of our results

345   relative to a random null. For all six models, the majority of the 999 permuted models failed to learn

346   associations between the response and predictor variables. The results of those that succeeded to fit a model to

347   completion (usually ca. 200 out of 999) are presented. The replicate and permuted BRT-models were compared

348   using various measures of model performance (above; nt, R^2_{pseudo} (Equation (4)), $R^2_{\mathrm{E-O}}$) and the ranks of

349   these values for each replicate BRT-model relative to the 999 permuted models for that region/scope.

3   Results

3.1   Describing environmental heterogeneity across scales

352   Across all variables considered, the Cape is more environmentally heterogeneousin the majority of pairwise

353   comparisons of grid-cells ($CLES > 0.50$, Mann-Whitney U-test: $P < 0.05$, Figure 1). The Cape is thus

354   more environmentally heterogeneous than SWA overall, but the degree to which it is more heterogeneous

355   varies between environmental variables. These effects also vary somewhat with the spatial scale concerned. In

356   some variables, the differentiation between Cape and SWA heterogeneity lessens at coarser scales (Figure 1b).

357   Indeed, when comparing the overall ranking and medians of Cape vs SWA roughness values for each variable,

358   we only find non-significant differences at the coarser 3QDS scale (Mann-Whitney U tests, $P > 0.05$, Figure

359   1b).

360   Most obviously, and as expected, topographic heterogeneity is greatest in the Cape (Figure 1). Though SWA

361   has a slightly wider distribution of elevational roughness values at coarse scales (e.g. 3QDS) compared to fine

362   scales (0.05º), so does the Cape. As such, the relative difference between the two regions seems invariant with

363   spatial scale ($CLES \approx 0.95$, Figure 1b). This concurs with our expectations, as the Cape is mountainous and

364   known to have steep elevational gradients (**???**), while SWA is much more topographically uniform.

365   Climatic heterogeneity presents less differentiation between the Cape and SWA than elevational roughness

366   (Figure 1a), though still the Cape predominates (Figure **??**b). Notably, the difference between Cape and SWA

367   mean annual rainfall and land surface temperature heterogeneity lessens when considered at coarse spatial

368   scales (3QDS scale, Figure **??**b). Rainfall seasonality (PDQ), however, is similarly more heterogeneous in the

369 Cape across all spatial scales considered.

370 Biological productivity, as measured by NDVI, varies spatially to a similar extent in the Cape and SWA (i.e. is
371 more similarly heterogeneous, $CLES < 0.60$, Figure 1).

372 Concerning edaphic variables, the Cape and SWA are similarly heterogeneous at coarser scales, particularly in
373 terms of CEC and Soil C (Figure 1b).

3.2 Comparing species turnover in the two regions

375 Following calculations of $\overline{J}_{\mathrm{QDS}}$ and T_{HDS} for each HDS-cell in each region, we used non-parametric
376 Mann-Whitney U-tests to compare the distributions of values in the Cape and SWA. The Cape possesses
377 generally greater floristic turnover than SWA, for both measures of turnover defined here ($P < 0.0001$, Figure
378 2a,b). Being derived from Jaccard distances, $\overline{J}_{\mathrm{QDS}}$ measures the average pairwise proportional floristic
379 turnover between QDS in each HDS. T_{HDS}, however, represents the latter of two partitionings of γ-diversity
380 (i.e. HDS-scale richness here): α- and β-diversity. As γ-diversity in the Cape is more greatly a function of
381 β-diversity than in SWA, the complement is necessarily true: γ-diversity in the Cape is less a function of
382 α-diversity than in SWA.

3.3 Predicting richness and turnover with environmental heterogeneity

384 Vascular plant species richness and turnover are found to both be predicted primarily by environmental
385 heterogeneity in the Cape (Figure 3a–c) and at least in-part by environmental heterogeneity in SWA (Figure
386 3d–f). Our six BRT-models performed adequately, and detected relationships between patterns of species
387 occurrence and the environment that do not occur by chance in the permuted datasets (Figures 4 and 3, Table 2).

388 BRT-models of species richness at the QDS-scale in each region seemed to generally performed best, as these
389 models had generally fit the greatest number of trees (nt, Figure 4a), and higher R^2-values (Figure 4b,c).
390 Notably, SWA models of species richness and turnover at the HDS-scale out-performed Cape models, while at
391 the QDS-scale the Cape models performed as-well or better (Figure 4, Table 3).

392 Across our BRT-models of species richness and turnover, the sets of environmental variables important to
393 model predictions differ substantially between the Cape and SWA, both in terms of which aspects of the
394 environment were found to be biologically relevant and in terms of the relative importance of absolute and

15

heterogeneity variables (Figure 3). Most obviously, species richness and turnover in the Cape are predicted in majority by environmental heterogeneity, which is not the case in SWA (piecharts inset Figure 3). Species richness and turnover in the Cape are predicted by a broad suite of environmental variables, with no individual variable contributing more than ca. 20% to any model prediction (Figure 3a–c). The SWA models' predictions, however, are largely determined by MAP (Figure 3d–f).

Species richness at QDS-scales, and to a lesser extent at HDS-scales, in the Cape is more predicted in large part by edaphic conditions (Figure 3a,b). Contrastingly, richness in SWA across both scales is mostly predicted by MAP and other climatic variables (Figure 3d,e).

Our BRT-models of species richness at QDS- and HDS-scales, in both regions, rank environmental variables somewhat differently (Figure 3a,b,d,e), though these differences are slightly less extreme than would be expected by chance ($P_{1-2} < 0.01$, Figure 5). This suggests a weak, but measurable, scale-dependence of the importance of different environmental variables in driving species richness.

It is noteworthy that BRT-models of species turnover (at HDS-scales) (Figure 3c,f) rank variables similarly to models of richness at HDS-scales ($P_{2-3} \leq 0.005$, Figure 5). This is likely due to the fact that species turnover is covaries with species richness. As such, though the signs of relationships determining turnover may differ from those determining richness, the importances of different variables would be similar.

4   Discussion

Conclusion: The Cape is more generally environmentally heterogeneous than the SWA, as expected (see prediction (i)). Though, there are cases where the SWA is arguably at-least-as-heterogeneous as the Cape, and we can observe here extreme regions of high edaphic heterogeneity, at fine scales, in SWA. These surpass the edaphic heterogeneity of the Cape, supporting our seventh prediction/conjecture.

We also have support for prediction (ii), as seen in Fig. **??**.

I have provided support for the hypothesis that the difference in plant species richness between the GCFR and SWAFR is accounted for by the fact that the GCFR is more abiotically heterogeneous than the SWAFR. As expected, the GCFR is shown to possess (i) a quantifiably more heterogeneous environment, and (ii) is heterogeneous at a finer spatial scale than the SWAFR. I have shown that vascular plant species richness (iii) can be explained in terms of environmental conditions, including environmental heterogeneity, in both the

GCFR and SWAFR. Also, I have shown that (iv) the set of environmental axes that explain plant species richness, both absolute and as heterogeneity, differs between the GCFR and SWAFR. These findings contribute towards an understanding of the ecological conditions that facilitate species coexistence (and likely stimulate ecological speciation) in these two regions.

These two regions present differentiable environmental spaces, each with heterogeneity varying across spatial scales. The clear separation of the regions' topographic features is as expected (Figures **??**A, **??**). Indeed, topography seems to be the most striking distinction between the regions. The Cape region has been found previously to have the second highest median topographic heterogeneity of the five Mediterranean-climate regions (Bradshaw & Cowling, 2014). The GCFR has a much wider range of scales exhibited in the heterogeneity across its environmental axes. Notably, each region has finer scale heterogeneity in some variables, and coarser scale in others—neither region is necessarily more fine or coarse than the other, as it depends on the variable concerned. BRT-models of species richness in both regions reveal species richness to depend on those environmental axes that differentiate the two regions (Figures **??**), **??**). The importance of variables is also shown to vary with spatial scale (Figure **??**), as previously suggested may be the case when modelling geographic patterns of biodiversity (Baudena et al., 2015). Indeed, as Cowling et al. (1996) describes differing patterns of species richness across spatial scales, so do the predictors of those patterns vary with scale (Hart et al., 2017).

The fact that a combination of absolute and roughness variables is also as predicted by the hypothesis in this study. In the models developed by Cramer & Verboom (2016) for South Africa, roughness in topography was largely superseded as an important predictor of species richness by other roughness variables. My models, however, did not show this. Similar to the study by Rensburg et al. (2002), my models revealed roughness in topography and other variables to be important. Although, Rensburg et al. (2002) considered differences within pixels, as opposed to this study, which considered differences between pixels. My models, those of Cramer & Verboom (2016), and those of Rensburg et al. (2002), do not all concur as to the role of roughness in elevation vs. more biologically meaningful variables in explaining species richness. The source of these discrepancies is unclear, though no doubt complex. The complements of environmental variables and methodologies used in these studies do differ, limiting extensive comparison between these analyses.

The determinants of vascular plant species are shown to be region specific (Figures **??**, **??**, **??**). The importance of MAP and roughness in rainfall seasonality (PCV) in predicting richness in the SWAFR (Figure **??**I, **??**J), aligns with the steep climatic gradients observed there (Cook et al., 2015). The soil variables that determine

17

452 plant species richness in the model for the SWAFR (Figures **??**K, **??**L) differ to those that determine richness in

453 the GCFR (Figures **??**G, **??**H), further highlighting the edaphic differences between these two regions.

454 Although both are nutrient leached systems, the SWAFR is flat, with soil-chronosequences (Laliberte et al.,

455 2014; Cook et al., 2015), while the GCFR is mountainous (Cowling et al., 1996; Cramer et al., 2014; Verboom

456 et al., 2017). The importance of roughness in soil density, and absolute texture, in the SWAFR (Figures **??**K,

457 **??**L) highlights the changes in soil that are associable with age of the substrate (e.g. particle size) as being

458 biologically relevant to species richness. The positive effect of soil clay content on species richness in the

459 SWAFR aligns with the findings of Laliberte et al. (2014) that richness in the SWAFR increases with soil age.

460 NDVI is more heterogeneous across the GCFR than the SWAFR (Figures **??**A). The fact that thermal variables

461 tend to be more rough in the GCFR (Figure **??**A) is likely due to possible covariance of the MODIS/Terra

462 products with topography, as MODIS data used here describes land surface temperature. As the GCFR is

463 topographically rugged, the roughness of NDVI may arise from this. Despite this, NDVI is an integrating

464 variable, which captures information about productivity, light availability, and soil nutrients (Power et al.,

465 2017). The fact that absolute NDVI contributes to predicting species richness in the GCFR, especially at finer

466 spatial scales (Figure **??**E) demonstrates the role of ecological productivity in facilitating the coexistence

467 diverse species assemblages. Environmental heterogeneity, then, is integral to explaining patterns of species

468 richness, but must be considered along with resource- and energy-availability axes. In so much as a diverse

469 environmental space supports more species, the materials and productivity required for biota to thrive are also

470 needed to support species (**???**; Gaston, 2000; Bøhn & Amundsen, 2004; Kreft & Jetz, 2007). As such, my

471 findings, along with those of previous studies (Rensburg et al., 2002; Thuiller et al., 2006; Kreft & Jetz, 2007;

472 Cramer & Verboom, 2016), suggest that there is ecological and evolutionary consequence to resource

473 availability *and* environmental heterogeneity, in that they tend to be positively associated with species richness.

474 The combined BRT-model of species richness for both regions reveals soil clay content as an important

475 predictor, at coarse spatial scales, despite this variable not being particularly important within each region

476 separately (Figure **??**). Though this model does not strictly consider the regions as separate, this finding may

477 indicate that the relationship between clay content and species richness differs between the regions. So far as

478 clay content can be used to predict species richness, it matters more to those predictions when applied to large

479 sections (i.e. coarse scales) of each regions.

480 Kreft & Jetz (2007) modelled global terrestrial vascular plant species richness, which focussed on primarily

481 absolute environmental values, underestimated the richness of the Cape flora. Though Kreft & Jetz (2007) did

include topographic heterogeneity in their predictor set, topography is often a proxy for more biologically meaningful variables (Cramer & Verboom, 2016). This explains why the inclusion of these variables (e.g. roughness in mean annual precipitation) yields more accurate predictions of species richness. Indeed, Thuiller et al. (2006) also included topographic heterogeneity. Cramer & Verboom (2016) described 68% of species richness at the QDS scale across South Africa. Regarding the GCFR, depending on whether one consults pseudo-R^2 (Table 3), the ratio of mean predicted to observed richness per grid-cell (Table 5), or the distributions of predicted vs. observed richness values per grid-cell (Figure **??**), I have achieved a similarly suitable level of predictive accuracy. There is, though, still unexplained species richness in light of my models. As Cramer & Verboom (2016), Rensburg et al. (2002), Thuiller et al. (2006), and Mouchet et al. (2015) have done, these macro-ecological models are a-historical. Evolutionary considerations of species richness in geographic space are worthwhile, especially in regions with environments stable over evolutionary time.

The findings here are correlative. There are, however, many proposed mechanisms to explain the correlative signals demonstrated here. My findings support the hypothesis that Mediterranean systems' plant species richness is a function of spatial variability in environmental conditions. This can stimulate diversification, and maintain that diversity by providing a range of habitats for species co-existence. Oligtrophic soils can stimulate an increase in functional diversity, through the evolution of diverse nutrient acquisition strategies (Lambers et al., 2010; Verboom et al., 2017) (e.g. sclerophylly (Cramer et al., 2014; Cook et al., 2015)). An aspect of the environment I have neglected to consider is fire, shown to also contribute to predictions here in the GCFR (Cramer & Verboom, 2016). Cardillo (2012) have shown the structuring forces behind species co-occurrence patterns, and thus likely species richness,differ between species-pairs with different post-fire responses and those with similar post-fire responses.

Though the GCFR was correctly predicted to have, on average, more species per grid-cell at HDS and 3QDS scales than the SWAFR, this was not the case for QDS grid-cells (Table 5). This demonstrates that the GCFR is indeed overall more rich in plant species than the SWAFR, but a given HDS in the SWAFR contains fewer species than a given GCFR HDS. Thus, the greater richness in the GCFR is a product of greater turnover in species at spatial scales no more coarse than the HDS. Species turnover is an interesting aspect to species richness studies, as it species turnover is implicit to species-area and co-existence-area relationships (Hart et al., 2017). One could expect patterns of endemism and species turnover to concur with patterns in environmental heterogeneity to some degree.

Following from the understanding that functionally diverse assemblages, which are more likely to be more

species rich, are likely to arise and/or occur in areas with diverse ecological pressures (Molina-Venegas et al., 2015), one would expect, then, heterogeneous habitats such as those in Mediterranean-type biodiversity hotspots to exhibit high levels functional beta diversity along steep environmental gradients (Molina-Venegas et al., 2015). If the niches concerning these functions are phylogenetically conserved among those biota, then one would also expect high levels of species and phylogenetic beta diversity along these gradients (Molina-Venegas et al., 2015). This concurs with the notion put forward by Power et al. (2017), wherein megadiverse systems such as these represent the results of "phylogenetic niche conservatism on a heterogeneous landscape". Thus, species and phylogenetic turnover should covary with environmental heterogeneity in some way. Indeed, endemism, at certain scales, could also follow this pattern. Thuiller et al. (2006) demonstrated that there is phylogenetic and biome related determinants of species richness. This makes sense, in light of the difficulty of crossing biome boundaries in Mediterranean systems (Power et al., 2017). NDVI and light availability, and the heterogeneity therein, are associated with high levels of floristic turnover (Power et al., 2017). This may be indicative of ecological specialisation precluding species from crossing these boundaries, thus increasing the level of endemism within a region, while also increasing the level of turnover, and thus likely species richness, along environmental gradients. Although, this may be debated. Beard et al. (2000) state that the high levels of endemism in SWAFR are function of habitat specialisation to soil mosaics. Cf. Laliberte et al. (2014), who say that this endemism is likely due to environmental filtering along these soil turnover sequences, as opposed to the juxtaposition of specialised species along soil gradients.

I have demonstrated support for the idea that environmental heterogeneity is positively associated with species richness, particularly Mediterranean systems. In the SWAFR and the GCFR, high levels of endemism and biodiversity are also likely the results of long-term landscape and climatic stability (Hopper, 1979). Thus, the roles of environmental variability through space, and stability through time, are the two main ways in which the environment relates to biodiversity in these regions.

Table captions

Captions are also repeated alongside their respective tables for readability.

Table 1: Georeferenced vascular plant species occurence and environmental data sources used in this study. Data were acquired for the Cape and SWA regions, with the temporal extent of data products used described where applicable. Abbreviations are as follows: MAP, mean annual precipitation; PDQ, precipitation in the

540 driest quarter; CEC, cation exchange capacity.

541 Table 2: Average percentile-ranks for BRT-model performance measures (nt, R^2_{pseudo} (Equation (4)), $R^2_{\text{E}-\text{O}}$)

542 of 1000 replicate BRT-models relative to 999 BRT-models fit to permuted datasets. Ranks approaching one

543 indicate that a set of replicate BRT-models had greater values than the permuted models.

544 Table 3: Estimated differences between replicate Cape and SWA BRT-models' performance measures (nt,

545 R^2_{pseudo} (Equation (4)), $R^2_{\text{E}-\text{O}}$) following t-tests. Positive values indicate that the Cape models had greater

546 values. In all cases, the Cape and SWA had highly significantly different values for these quality measures

547 ($P < 0.0001$).

Figure captions

549 Captions are also repeated alongside their respective figures for readability.

550 Figure 1: Types of environmental heterogeneity, compared between the the Cape and SWA—namely for (a)

551 elevation, (b) climatic variables, (c) NDVI and (d) soil variables—in each panel consisting of three sub-panels

552 per variable type. The upper row of panels shows example distributions of roughness values (Equation (1)),

553 showing the different extremes in environmental heterogeneity observed in each region when compared at fine

554 (0.05º) and coarse (3QDS) scales. Each distribution has under it an area of one. Histograms were constructed

555 using 20 breaks. In the lower row of panels, these distributions of roughness values were compared between

556 the Cape and SWA at each of the four spatial scales, not just 0.05º and 3QDS, using non-parametric

557 Mann-Whitney U-tests to test for differences. The "common language effect size" ($CLES$, see text) describes

558 these differences (b). U-tests for almost all environmental variables yielded significant differences ($P < 0.05$)

559 between Cape and SWA values (NS, non-significant differences). CLES for 0.05 res. is for 5000 random cells

560 in each region, as the Mann-Whitney U-test cannot handle more than a few thousand values per sample when

561 comparing.

562 Figure 2: Species turnover, described in two forms ((a) mean Jaccard distance between QDS in each HDS

563 ($\overline{J}_{\text{QDS}}$), (b) additively defined turnover (T_{HDS}, Equation (2)) as a proportion of HDS richness (S_{HDS})),

564 compared between the Cape and SWA. Mann-Whitney U-tests between the Cape and SWA distributions of

565 $\overline{J}_{\text{QDS}}$ and T_{HDS} yielded significant differences.

566 Figure 3: Relative influence of environmental variables (including heterogeneity variables—prefixed with "R")

21

567 in boosted regression tree (BRT) model predictions for the final six models' response variables in Greater Cape

568 Floristic Region (Cape) and Southwest Australia Floristic Region (SWA): vascular plant species richness at the

569 (b,e) QDS-scale, (a,d) HDS-scale and (c,f) turnover $(= \overline{J}_{\mathrm{QDS}})$. All BRT-models were permitted to fit

570 three-way interactions between environmental variables. Points denote the average contribution of an

571 environmental variable to model-predictions across the 1000 replicate BRT-models for that region/scope.

572 Horizontal ticks denote the average for the 999 permuted BRT-models. The standard deviations above and

573 below these means are shown with vertical lines. Note that in the case of the replicate models they are very

574 small in most cases, obsfucating them. Colour represents the general category of the environment (keyed) to

575 which a variable belongs, as in Figure 1b. Piecharts inset display the same information (left-most piecharts),

576 and additionally grouped according to whether a variable was absolute or roughness-transformed (right-most

577 piecharts). F-statistics inset are for one-way ANOVAs of differences in variables' relative influences from the

578 replicate $(F_{\mathrm{rep.}})$ and permuted $(F_{\mathrm{prm.}})$ BRT-models.

579 Figure 4: Distributions of three measures of boosted regression tree (BRT) model performance (a) the number

580 of trees in the model nt, (b) R^2_{pseudo} (Equation (4)), (c) $R^2_{\mathrm{E-O}}$ (see text). These measures are presented for the

581 six sets of permuted (pale bars) and six sets of replicate BRT-models (dark bars) as in Figure 3, coloured

582 according to the region of interest as in Figures 1a and 2. In all cases, replicate BRT-models almost entirely

583 out-rank the permuted models in terms of performance (Table 2) and Cape and SWA models had significantly

584 different values for each metric (Table 3). Note, the actual differences between Cape and SWA models' values

585 is not realistically important in some cases.

586 Figure 5: Differences in the rankings of environmental variables' (including heterogeneity variables) relative

587 influences on boosted regression tree (BRT) model predictions of vascular plant species richness and turnover

588 in (a) Cape and (b) SWA (as in Figure 3). Each point represents an environmental variable's rank in

589 BRT-model importance, decreasing in importance from left to right. Rankings used here are the same as that of

590 the average relative influence for variables across replicate BRT-models, presented in Figure 3. Coloured lines

591 connect points representing the same environmental variable. Points' outlines are coloured according to the

592 general category of the environment (keyed) to which a variable belongs, as in Figuress 1b and 3, while points'

593 centres are coloured according to whether a variable was roughness-transformed or not. The comparisons of

594 variables' rankings of interest are between QDS- and HDS-scale richness (rows nos. 1 and 2) and between

595 HDS-scale richness and turnover (rows nos. 2 and 3). Statistics (Δ- and P-values) inset at the top and bottom

596 of each panel refer to these comparisons respectively. Δ-values represent the average absolute difference in

597 ranks across variables between two models' rankings. The associate P-value results from ranking the observed

598 Δ-values against 999 Δ-values based on random permutations of variables' rankings (SI1), such that more

599 significant P-values denote rankings more similar than would be expected by chance.

References

601 Baudena, M., Sánchez, A., Georg, C.-P., Ruiz-Benito, P., Rodríguez, M.Á., Zavala, M.A., & Rietkerk, M. (2015) Revealing patterns of
602   local species richness along environmental gradients with a novel network tool. *Scientific Reports*, **5**, 11561.

603 Beard, J.S., Chapman, A.R., & Gioia, P. (2000) Species richness and endemism in the Western Australian flora. *Journal of
604   Biogeography*, **27**, 1257–1268.

605 Bradshaw, P.L. & Cowling, R.M. (2014) Landscapes, rock types, and climate of the Greater Cape Floristic Region. *Fynbos: Ecology,
606   evolution and conservation of a megadiverse region* (ed. by N. Allsopp, J.F. Colville, and G.A. Verboom), pp. 26–46.
607   Oxford University Press, Oxford.

608 Bøhn, T. & Amundsen, P.-A. (2004) Ecological Interactions and Evolution: Forgotten Parts of Biodiversity? *BioScience*, **54**, 804.

609 Cardillo, M. (2012) The phylogenetic signal of species co-occurrence in high-diversity shrublands: different patterns for fire-killed and
610   fire-resistant species. *BMC Ecology*, **12**, 21.

611 Cook, L.G., Hardy, N.B., & Crisp, M.D. (2015) Three explanations for biodiversity hotspots: small range size, geographical overlap
612   and time for species accumulation. An Australian case study. *New Phytologist*, **207**, 390–400.

613 Cowling, R.M., Rundel, P.W., Lamont, B.B., Arroyo, M.K., & Arianoutsou, M. (1996) Plant diversity in mediterranean-climate regions.
614   *Trends in Ecology and Evolution*, **11**, 362–366.

615 Cramer, M.D. & Verboom, G.A. (2016) Measures of biologically relevant environmental heterogeneity improve prediction of regional
616   plant species richness. *Journal of Biogeography*, 1–13.

617 Cramer, M.D., West, A.G., Power, S.C., Skelton, R., & Stock, W.D. (2014) Plant ecophysiological diversity. *Fynbos: Ecology,
618   evolution and conservation of a megadiverse region* pp. 248–272. Oxford University Press, Oxford.

619 Deblauwe, V., Droissart, V., Bose, R., Sonké, B., Blach-Overgaard, A., Svenning, J.C., Wieringa, J.J., Ramesh, B.R., Stévart, T., &
620   Couvreur, T.L.P. (2016) Remotely sensed temperature and precipitation data improve species distribution modelling in the
621   tropics. *Global Ecology and Biogeography*, **25**, 443–454.

622 Elith, J., Leathwick, J.R., & Hastie, T. (2008) A working guide to boosted regression trees. *Journal of Animal Ecology*, **77**, 802–813.

623 Farr, T., Rosen, P., Caro, E., Crippen, R., Duren, R., Hensley, S., Kobrick, M., Paller, M., Rodriguez, E., Roth, L., Seal, D., Shaffer, S.,
624   Shimada, J., Umland, J., Werner, M., Oskin, M., Burbank, D., & Alsdorf, D. (2007) The shuttle radar topography mission.
625   *Reviews of Geophysics*, **45**, 1–33.

626   Funk, C.C., Peterson, P.J., Landsfeld, M., Pedreros, D.H., Verdin, J., Shukla, S., Husak, G., Rowland, J.D., Harrison, L., Hoell, A., &

627   Michaelsen, J. (2015) The climate hazards infrared precipitation with stations—a new environmental record for monitoring

628   extremes. *Scientific Data*, **2**, 150066.

629   Gaston, K.J. (2000) Global patterns in biodiversity. *Nature*, **405**, 220–227.

630   GBIF (24 July 2017) GBIF Occurrence Download..

631   GBIF (24 July 2017) GBIF Occurrence Download..

632   Gioia, P. & Hopper, S.D. (2017) A new phytogeographic map for the Southwest Australian Floristic Region after an exceptional decade

633   of collection and discovery. *Botanical Journal of the Linnean Society*, **184**, 1–15.

634   Hart, S.P., Usinowicz, J., & Levine, J.M. (2017) The spatial scales of species coexistence. *Nature Ecology & Evolution*, **1**, 1066–1073.

635   Hengl, T., Mendes de Jesus, J., Heuvelink, G.B.M., Ruiperez Gonzalez, M., Kilibarda, M., Blagoti?, A., Shangguan, W., Wright, M.N.,

636   Geng, X., Bauer-Marschallinger, B., Guevara, M.A., Vargas, R., MacMillan, R.A., Batjes, N.H., Leenaars, J.G.B., Ribeiro, E.,

637   Wheeler, I., Mantel, S., & Kempen, B. (2017) SoilGrids250m: Global gridded soil information based on machine learning.

638   *PLoS ONE*, **12**, e0169748.

639   Hopper, S.D. (1979) Biogeographical Aspects of Speciation in the Southwest Australian Flora. *Annual Review of Ecology and*

640   *Systematics*, **10**, 399–422.

641   Hopper, S.D. & Gioia, P. (2004) The Southwest Australian Floristic Region: Evolution and Conservation of a Global Hot Spot of

642   Biodiversity. *Annual Review of Ecology, Evolution, and Systematics*, **35**, 623–650.

643   Kreft, H. & Jetz, W. (2007) Global patterns and determinants of vascular plant diversity. *Proceedings of the National Academy of*

644   *Sciences*, **104**, 5925–5930.

645   Laliberte, E., Zemunik, G., & Turner, B.L. (2014) Environmental filtering explains variation in plant diversity along resource gradients.

646   *Science*, **345**, 1602–1605.

647   Lambers, H., Brundrett, M.C., Raven, J.A., & Hopper, S.D. (2010) Plant mineral nutrition in ancient landscapes: high plant species

648   diversity on infertile soils is linked to functional diversity for nutritional strategies. *Plant and Soil*, **334**, 11–31.

649   Larsen, R., Holmern, T., Prager, S.D., Maliti, H., & Røskaft, E. (2009) Using the extended quarter degree grid cell system to unify

650   mapping and sharing of biodiversity data. *African Journal of Ecology*, **47**, 382–392.

651   Levin, L.A., Sibuet, M., Gooday, A.J., Smith, C.R., & Vanreusel, A. (2010) The roles of habitat heterogeneity in generating and

652   maintaining biodiversity on continental margins: an introduction. *Marine Ecology*, **31**, 1–5.

653   Lobo, J.M., Jay-robert, P., Lumaret, J.-p., Lobo, J.M., Jay-robert, P., & Lumaret, J.-p. (2004) Modelling the Species Richness

654   Distribution for French Aphodiidae (Coleoptera, Scarabaeoidea). *Ecography*, **27**, 145–156.

655   Mateo, R.G., Mokany, K., & Guisan, A. (2017) Biodiversity Models: What If Unsaturation Is the Rule? *Trends in Ecology &*

656 *Evolution*, **32**, 556–566.

657 Molina-Venegas, R., Aparicio, A., Slingsby, J.A., Lavergne, S., & Arroyo, J. (2015) Investigating the evolutionary assembly of a
658 Mediterranean biodiversity hotspot: Deep phylogenetic signal in the distribution of eudicots across elevational belts. *Journal*
659 *of Biogeography*, **42**, 507–518.

660 Mouchet, M., Levers, C., Zupan, L., Kuemmerle, T., Plutzar, C., Erb, K., Lavorel, S., Thuiller, W., & Haberl, H. (2015) Testing the
661 effectiveness of environmental variables to explain European terrestrial vertebrate species richness across biogeographical
662 scales. *PLoS ONE*, **10**, 1–16.

663 Mucina, L. & Rutherford, M.C. (2006) *The vegetation of South Africa, Lesotho and Swaziland.* South African National Biodiversity
664 Institute,

665 NIMA (2000) Amendment 1. 3 January 2000. Department of Defense World Geodetic System 1984. Its Definition and Relationships
666 with Local Geodetic Systems. 1–3.

667 Olson, D.M., Dinerstein, E., Wikramanayake, E.D., Burgess, N.D., Powell, G.V.N., Underwood, E.C., D'amico, J.A., Itoua, I., Strand,
668 H.E., Morrison, J.C., & Others (2001) Terrestrial Ecoregions of the World: A New Map of Life on Earth: A new global map of
669 terrestrial ecoregions provides an innovative tool for conserving biodiversity. *BioScience*, **51**, 933–938.

670 Power, S.C., Verboom, G.A., Bond, W.J., & Cramer, M.D. (2017) Environmental correlates of biome-level floristic turnover in South
671 Africa. *Journal of Biogeography*, **44**, 1745–1757.

672 R Core Team (2018) *R: A Language and Environment for Statistical Computing. Version 3.5.0.* R Foundation for Statistical
673 Computing, Vienna, Austria.

674 Rensburg, B.J. van, Chown, S.L., & Gaston, K.J. (2002) Species Richness, Environmental Correlates, and Spatial Scale: A Test Using
675 South African Birds. *The American Naturalist*, **159**, 566–577.

676 Ricklefs, R.E. (1987) Community diversity: relative roles of local and regional processes. *Science, New Series*, **235**, 167–171.

677 Thuiller, W., Midgley, G.F., Rouget, M., Cowling, R.M., F. Midgley, G., Rougeti, M., & M. Cowling, R. (2006) Predicting patterns of
678 plant species richness in megadiverse South Africa. *Ecography*, **29**, 733–744.

679 Verboom, G.A., Stock, W.D., & Cramer, M.D. (2017) Specialization to extremely low-nutrient soils limits the nutritional adaptability
680 of plant lineages. *The American Naturalist*, **In press**,.

681 Wardell-Johnson, G. & Horwitz, P. (1996) Conserving biodiversity and the recognition of heterogeneity in ancient landscapes: a case
682 study from south-western Australia. *Forest Ecology and Management*, **85**, 219–238.

Biosketches

Ruan van Mazijk is currently a Masters student at the University of Cape Town, interested in phylogenetic systematics, macroecology, community and functional ecology.

Michael D. Cramer

G. Anthony Verboom

Author contributions

MDC and GAV conceived the study question, which RVM investigated under their supervision for his BSc Hons project. The analyses and programming work were largely devised by RVM, with input from the other authors, and was carried out by RVM. RVM wrote the first draft of the manuscript and all authors contributed equally thereafter.

Tables

Table 1: Georeferenced vascular plant species occurence and environmental data sources used in this study. Data were acquired for the Cape and SWA regions, with the temporal extent of data products used described where applicable. Abbreviations are as follows: MAP, mean annual precipitation; PDQ, precipitation in the driest quarter; CEC, cation exchange capacity.

Variable	Source	Temporal extent	Citation
Plant species occurrences	GBIF	TODO	**??, ??**
Elevation	SRTM v2.0		**??**
NDVI	MODIS (MOD13C2)	Feb. 2000 to Apr. 2017	**??**
Climatic variables			
Surface temperature	MODIS (MOD11C3)	Feb. 2000 to Apr. 2017	**??**
MAP	CHIRPS v2.0	Jan. 1981 to Feb. 2017	**??**
PDQ	CHIRPS v2.0	Jan. 1981 to Feb. 2017	**??**
Soil variables			
CEC	SoilGrids250m (CECSOL M 250m)		**??**
Clay	SoilGrids250m (CLYPPT M 250m)		
Soil C	SoilGrids250m (OCDENS M 250m)		
pH	SoilGrids250m (PHIKCL M 250m)		

Table 2: Average percentile-ranks for BRT-model performance measures (nt, R^2_{pseudo} (Equation (4)), $R^2_{\text{E-O}}$) of 1000 replicate BRT-models relative to 999 BRT-models fit to permuted datasets. Ranks approaching one indicate that a set of replicate BRT-models had greater values than the permuted models.

Model	nt	R^2_{pseudo}	R^2_{E-O}
QDS-richness			
GCFR	1.000	1.000	1.000
SWAFR	1.000	1.000	1.000
HDS-richness			
GCFR	0.987	1.000	0.988
SWAFR	1.000	1.000	1.000
HDS-turnover			
GCFR	0.977	0.992	0.979
SWAFR	0.997	1.000	1.000

Table 3: Estimated differences between replicate Cape and SWA BRT-models' performance measures (nt, R^2_{pseudo} (Equation (4)), $R^2_{\text{E-O}}$) following t-tests. Positive values indicate that the Cape models had greater values. In all cases, the Cape and SWA had highly significantly different values for these quality measures ($P < 0.0001$).

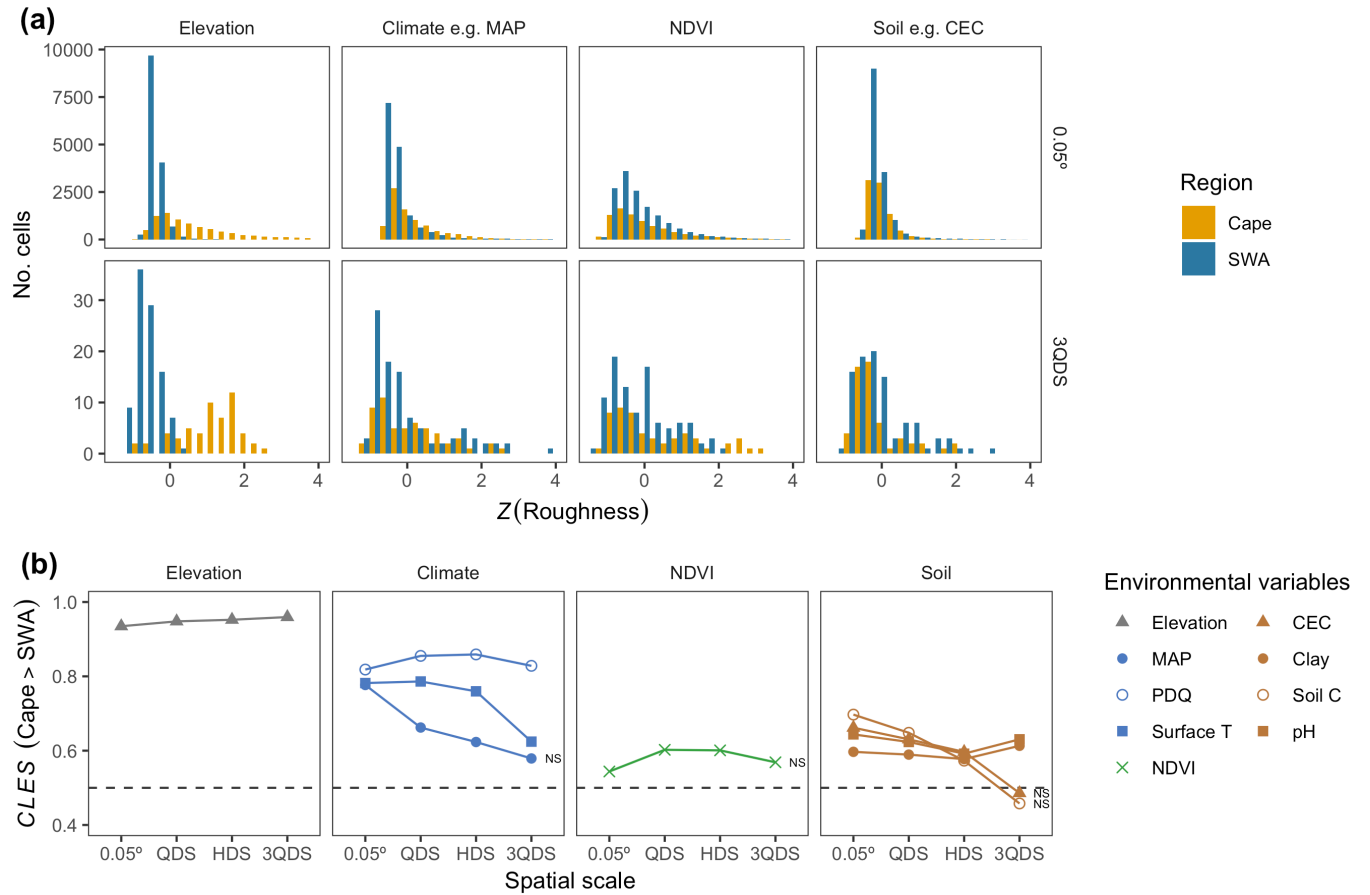| Model	nt	R^2_{pseudo}	$R^2_{\text{E-O}}$
QDS-richness	542.938	0.063	-0.005
HDS-richness	-808.994	-0.064	-0.233
HDS-turnover	-997.045	-0.052	-0.296

Figures

Figure 1: Types of environmental heterogeneity, compared between the the Cape and SWA—namely for (a) elevation, (b) climatic variables, (c) NDVI and (d) soil variables—in each panel consisting of three sub-panels per variable type. The upper row of panels shows example distributions of roughness values (Equation (1)), showing the different extremes in environmental heterogeneity observed in each region when compared at fine (0.05º) and coarse (3QDS) scales. Each distribution has under it an area of one. Histograms were constructed using 20 breaks. In the lower row of panels, these distributions of roughness values were compared between the Cape and SWA at each of the four spatial scales, not just 0.05º and 3QDS, using non-parametric Mann-Whitney U-tests to test for differences. The "common language effect size" ($CLES$, see text) describes these differences (b). U-tests for almost all environmental variables yielded significant differences ($P < 0.05$) between Cape and SWA values (NS, non-significant differences). CLES for 0.05 res. is for 5000 random cells in each region, as the Mann-Whitney U-test cannot handle more than a few thousand values per sample when comparing.
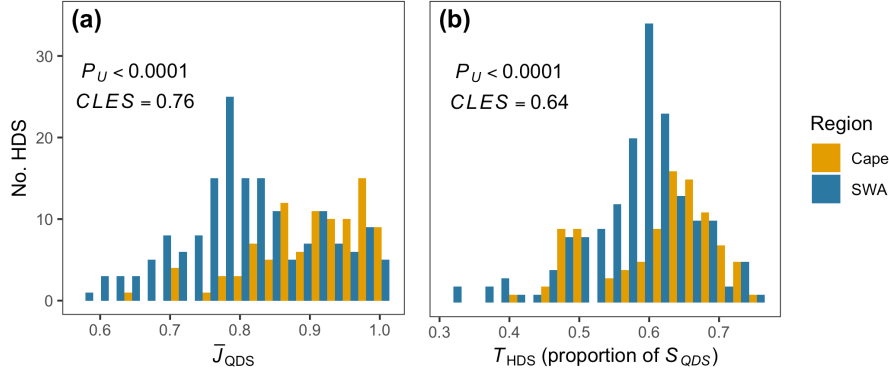
Figure 2: Species turnover, described in two forms ((a) mean Jaccard distance between QDS in each HDS ($\overline{J}_{\mathrm{QDS}}$), (b) additively defined turnover (T_{HDS}, Equation (2)) as a proportion of HDS richness (S_{HDS})), compared between the Cape and SWA. Mann-Whitney U-tests between the Cape and SWA distributions of $\overline{J}_{\mathrm{QDS}}$ and T_{HDS} yielded significant differences.
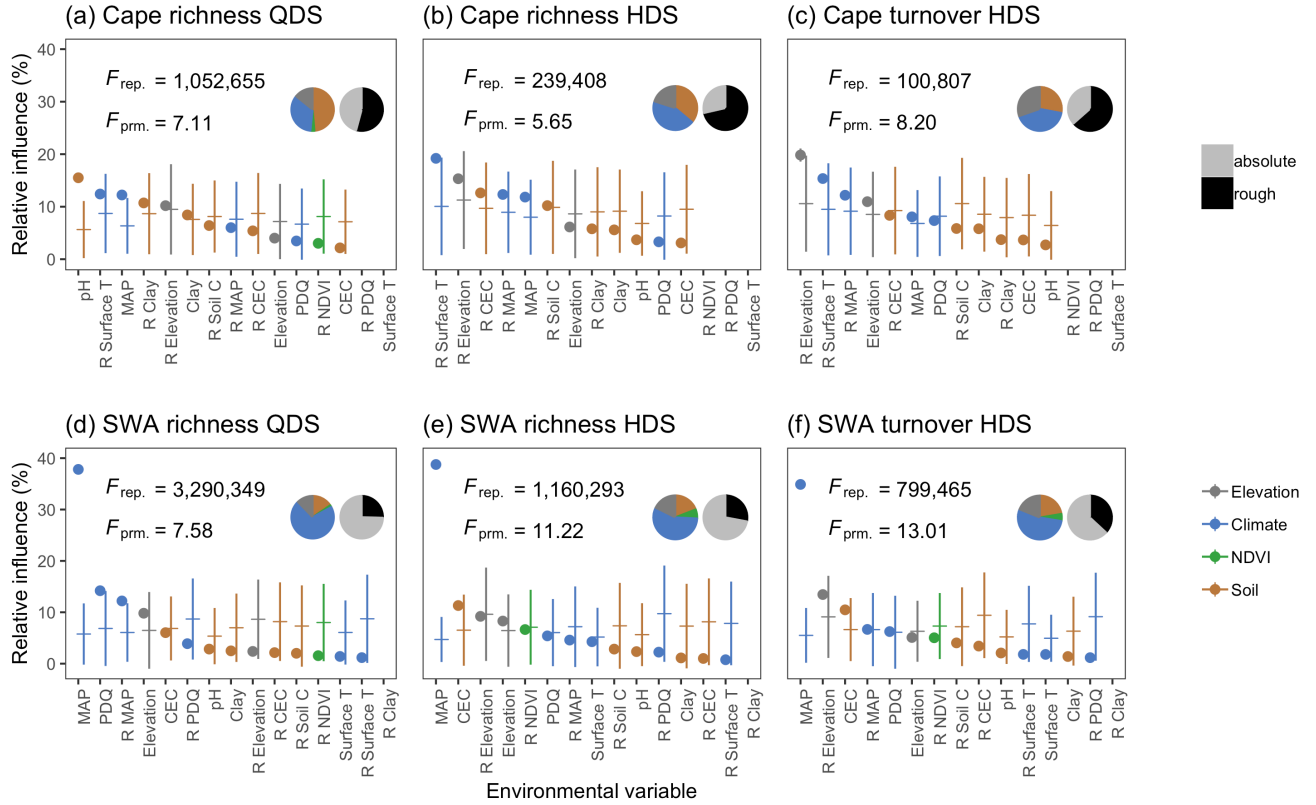
Figure 3: Relative influence of environmental variables (including heterogeneity variables—prefixed with "R") in boosted regression tree (BRT) model predictions for the final six models' response variables in Greater Cape Floristic Region (Cape) and Southwest Australia Floristic Region (SWA): vascular plant species richness at the (b,e) QDS-scale, (a,d) HDS-scale and (c,f) turnover ($= \overline{J}_{\mathrm{QDS}}$). All BRT-models were permitted to fit three-way interactions between environmental variables. Points denote the average contribution of an environmental variable to model-predictions across the 1000 replicate BRT-models for that region/scope. Horizontal ticks denote the average for the 999 permuted BRT-models. The standard deviations above and below these means are shown with vertical lines. Note that in the case of the replicate models they are very small in most cases, obsfucating them. Colour represents the general category of the environment (keyed) to which a variable belongs, as in Figure 1b. Piecharts inset display the same information (left-most piecharts), and additionally grouped according to whether a variable was absolute or roughness-transformed (right-most piecharts). F-statistics inset are for one-way ANOVAs of differences in variables' relative influences from the replicate ($F_{\mathrm{rep.}}$) and permuted ($F_{\mathrm{prm.}}$) BRT-models.
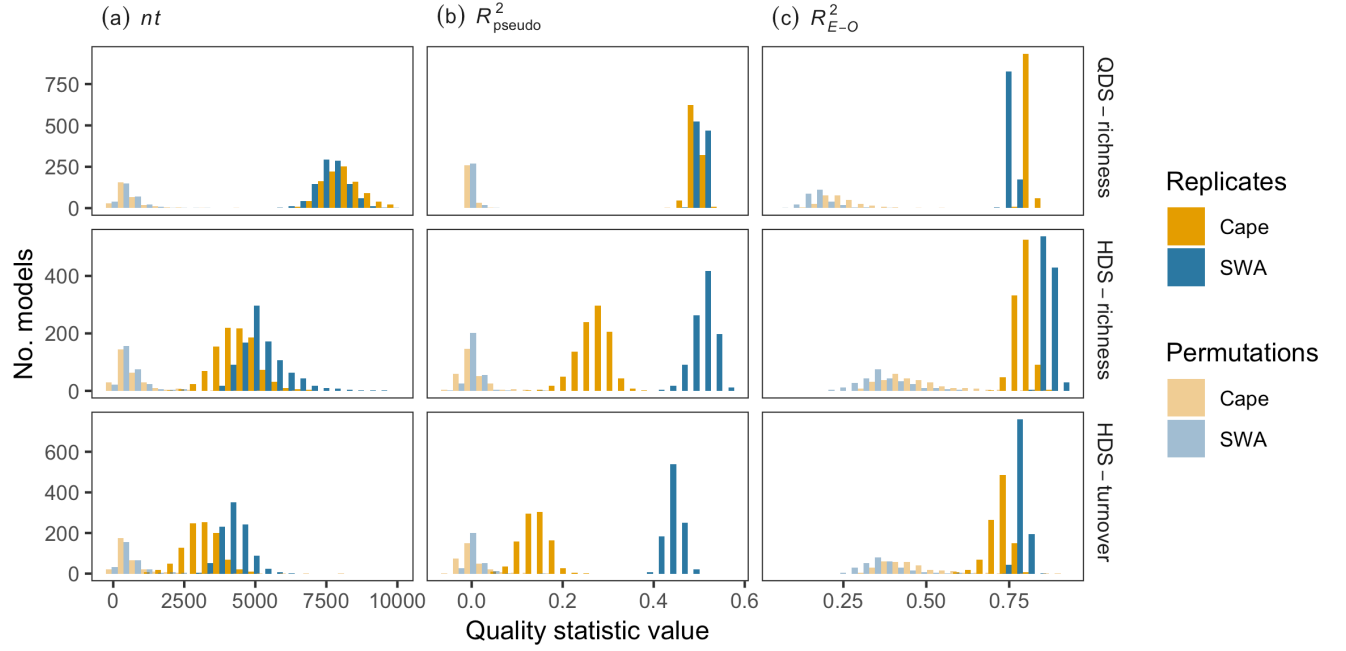
31

Figure 4: Distributions of three measures of boosted regression tree (BRT) model performance (a) the number of trees in the model nt, (b) R^2_{pseudo} (Equation (4)), (c) $R^2_{\text{E}-\text{O}}$ (see text). These measures are presented for the six sets of permuted (pale bars) and six sets of replicate BRT-models (dark bars) as in Figure 3, coloured according to the region of interest as in Figures 1a and 2. In all cases, replicate BRT-models almost entirely out-rank the permuted models in terms of performance (Table 2) and Cape and SWA models had significantly different values for each metric (Table 3). Note, the actual differences between Cape and SWA models' values is not realistically important in some cases.
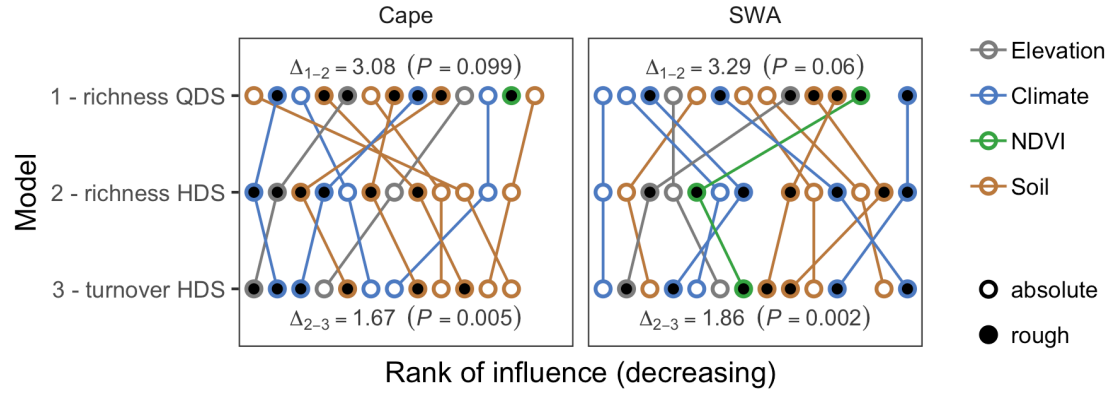
Figure 5: Differences in the rankings of environmental variables' (including heterogeneity variables) relative influences on boosted regression tree (BRT) model predictions of vascular plant species richness and turnover in (a) Cape and (b) SWA (as in Figure 3). Each point represents an environmental variable's rank in BRT-model importance, decreasing in importance from left to right. Rankings used here are the same as that of the average relative influence for variables across replicate BRT-models, presented in Figure 3. Coloured lines connect points representing the same environmental variable. Points' outlines are coloured according to the general category of the environment (keyed) to which a variable belongs, as in Figuress 1b and 3, while points' centres are coloured according to whether a variable was roughness-transformed or not. The comparisons of variables' rankings of interest are between QDS- and HDS-scale richness (rows nos. 1 and 2) and between HDS-scale richness and turnover (rows nos. 2 and 3). Statistics (Δ- and P-values) inset at the top and bottom of each panel refer to these comparisons respectively. Δ-values represent the average absolute difference in ranks across variables between two models' rankings. The associate P-value results from ranking the observed Δ-values against 999 Δ-values based on random permutations of variables' rankings (SI1), such that more significant P-values denote rankings more similar than would be expected by chance.